MATERIALS PHYSICS AND MECHANICS RESEACH ARTICLE

Submitted: June 4, 2024 **Revised: June 20, 2024** **Accepted: July 8, 2024**

Outstanding ductility of high-strength ultrafine-grained aluminium at cryogenic temperatures

T.S. Orlova ✉, **D.I. Sadykov**

Ioffe Institute, St. Petersburg, Russia

✉ orlova.t@mail.ioffe.ru

ABSTRACT

By decreasing the temperature of the tensile tests from 293 to 77 K, a drastic increase in ductility (elongation to failure ~ 40 % and uniform elongation ~ 25 %) was demonstrated for the first time, along with an increase in strength (yield stress ~ 235 MPa and ultimate tensile strength ~ 265 MPa) for ultrafine-grained aluminium structured by combination of equal-channel angular pressing and cold rolling with subsequent annealing. The increase in ductility at 77 K is accompanied by an increase in the strain hardening coefficient. The physical reasons for the significant increase in ductility at 77 K are discussed in comparison with the peculiarities of microstructure. The obtained combination of ductility and strength opens up prospects for the use of this material at cryogenic temperatures, as well as the application of cryogenic temperatures for the formation of its products of complex shapes.

KEYWORDS

aluminium • ultrafine-grained structure • ductility • strength • cryogenic temperatures

Citation: Orlova TS, Sadykov DI. Outstanding ductility of high-strength ultrafine-grained aluminium at cryogenic temperatures. *Materials Physics and Mechanics*. 2024;52(3): 73–79.
http://dx.doi.org/10.18149/MPM.5232024_7

Introduction

Grain refinement by severe plastic deformation (SPD) methods is widely used to increase the strength of aluminium and its alloys [1–6]. As a result of such processing, an ultrafine-grained (UFG) structure is formed, with an average grain size usually ranging from 100 to 1000 nm, depending on the SPD method used, processing parameters, and the chemical composition of the specific alloy [1]. The most widely used SPD methods currently are equal-channel angular pressing (ECAP), high-pressure torsion (HPT), and accumulative roll bonding [1,3,7–9]. The formation of UFG structure leads to a significant (several times) increase in strength, however, ductility is significantly reduced [1,7,10]. The reduction in ductility greatly complicates the processing of such materials and, consequently, limits their industrial application. The traditional method for increasing ductility is a suitable annealing at specific temperatures and durations. However, the increase in ductility in this case is accompanied by grain growth and, consequently, leads to significant decrease in strength [11,12]. The thermal stability of UFG materials decreases with increase in their chemical purity and decrease in grain size, which leads to decrease in strength when using, for example, hot pressing for the manufacture of products from them. Previously, we suggested a new approach to achieve significant increase in ductility at room temperature (RT) while maintaining high strength of UFG Al (99.6 wt. %), structured by the HPT method [13]. This approach presents the use of a special deformation-heat treatment (DHT), consisting of low-temperature annealing and

Publisher: Peter the Great St. Petersburg Polytechnic University

additional small HPT deformation at RT. As a result of such DHT, a good combination of strength (yield stress $\sigma_{0.2}$ ~ 130 MPa and ultimate tensile strength σ_{UTS} ~ 180 MPa) and ductility (elongation to failure δ ~ 34 % and uniform elongation δ_1 ~ 19 %) at RT was achieved for HPT Al [14]. As was shown, the increase in ductility of HPT Al after such DHT is due to increase in the degree of non-equilibrium of high-angle grain boundaries through their relaxation and subsequent introduction of additional density of extrinsic dislocations into them [15,16]. However, such DHT did not ensure high ductility in UFG Al, in which the UFG structure was formed by a combination of ECAP and cold rolling (CR) methods [17]. As a result of structuring aluminium by the combination of ECAP and CR methods with subsequent annealing at 150 °C for 1 h, remarkable strength ($\sigma_{0.2}$ ~ 182 MPa, σ_{UTS} ~ 212 MPa) was achieved and thermal stability of properties up to 150 °C, at least [17]. At the same time, δ was equal to ~ 9.6 %, and δ_1 was only ~ 1.2 %, indicating low formability of this material at RT.

In the present work, it has been shown that deformation at cryogenic temperatures (77 K) of samples structured by the combination of ECAP and CR methods followed by annealing (T = 150 °C, t = 1 h), provides a drastic increase in ductility accompanied by increase in strength. The achieved ductility, primarily uniform elongation, indicate the prospects of using Al structured in this way for products operating at low temperatures, as well as for deformation treatments of this material under cryogenic temperature conditions.

Materials and Methods

Commercially pure Al (A7E, 99.7 wt. % Al) was chosen for the study. The UFG structure was formed by combination of ECAP (4 passes, via route B_C, the angle between channels is 90°) and CR (total thickness reduction ~ 90 %), followed by annealing at T = 150 °C for 1 h (Al_ECAP+CR+AN state). Mechanical properties were studied by uniaxial tensile tests using the blade-shaped samples with a gauge size of 2.0 × 1.0 × 6.0 mm^3 (the gauge length was oriented along the rolling direction). Tensile tests were carried out on a Shimadzu AG-50kNX testing machine with a constant strain rate of 5 × 10^{-4} s^{-1} at RT, as well as in liquid nitrogen (at 77 K). At least three samples were tested for each state and temperature. The yield stress ($\sigma_{0.2}$), ultimate tensile strength (σ_{UTS}), elongation to failure (δ) and uniform elongation (δ_1) were determined from the obtained stress-strain curves. The microstructure of samples was studied by transmission electron microscopy (TEM) using a JEOL 2100 microscope at an accelerating voltage of 200 kV. TEM studies were carried out in the plane marked in red in Fig. 1(a), which is formed by the rolling direction (RD) and the direction normal to the rolling plane (ND). Analysis of the obtained microstructure images was carried out using ImageJ software. Samples for TEM studies were prepared by mechanical polishing followed by twin-jet electropolishing in solution of nitric acid (25 %) in methanol at -25 °C at an operating voltage of 25 V.

Results and Discussion

A typical TEM image of the microstructure is shown in Fig. 1(a). Based on a series of TEM images obtained, grain sizes were measured using ImageJ software. The size of each grain was determined by estimating the diameter of a circle equivalent in area to each individual grain. The grain size distribution obtained on the basis of ~ 100 grains is shown in Fig. 1(b). The average grain size is (d_G) ~ 665 nm. According to data obtained by electron backscatter diffraction, such structure contains predominantly (67 %) high-angle grain boundaries [17]. Despite the annealing at 150 °C, dislocations are clearly visible in some grains (Fig. 1(a)). According to X-ray diffraction analysis, the dislocation density in the Al_ECAP+CR+AN state is ~ 1.6×10^{12} m^{-2} [17].

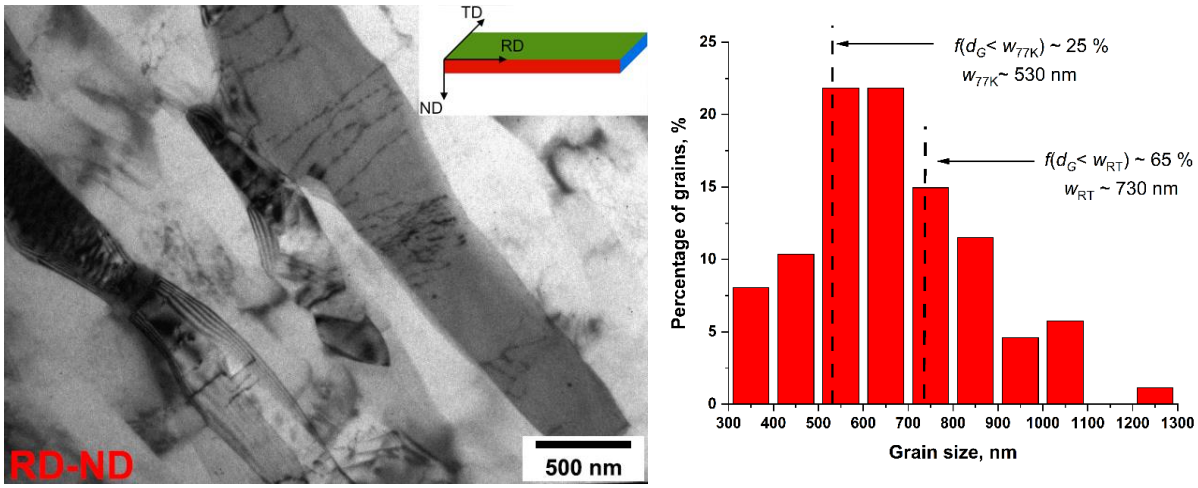

(a) (b)

Fig. 1. (a) – typical TEM image of Al_ECAP+CR+AN samples in RD-ND plane with indication of the sample orientation relative to the rolling direction RD; ND and TD - normal and transverse directions, respectively; (b) – statistical grain size distribution for Al_ECAP+CR+AN. w_{RT}, w_{77K} – the steady-state subgrain size at RT and 77 K, respectively (see the explanation in the text); f ($d_G < w_{RT}$), f ($d_G < w_{77K}$) – fractions of grains with the grain size d_G smaller than w_{RT}, and w_{77K}, respectively

Figure 2 shows the stress-strain curves of the Al_ECAP+CR+AN samples at RT and 77 K. For comparison, the stress-strain curve of Al in the initial coarse-grained state (CG) at RT is also presented. The mechanical characteristics of the Al_ECAP+CR+AN samples at RT are similar to those we obtained previously [17]. As is seen (Fig. 2), the strength characteristics of the material in the UFG state Al_ECAP+CR+AN significantly exceed those in the initial CG state. In the UFG state, compared to the CG state, the value of $\sigma_{0.2}$ increased from ~ 35 to ~ 185 MPa, and the value of σ_{UTS} increased from ~ 50 to ~ 215 MPa. The value of δ at RT drops by 4 times, from ~ 40 % in the CG state to δ ~ 10 % in the UFG state. The uniform elongation becomes very low (δ_1 ~ 1 %), which indicates the localization of deformation in UFG Al immediately after the onset of plastic flow. However, the Al_ECAP+CR+AN samples demonstrate excellent ductility at 77 K (curve 3 in Fig. 2): δ reaches ~ 40 %, and uniform elongation is ~ 25 %, which exceeds δ_1 at RT by ~ 25 times. The increase in ductility of UFG Al at 77 K is accompanied by a noticeable increase in the strength (by ~ 1.3 times). The values of $\sigma_{0.2}$ and σ_{UTS} increased from ~ 185 to ~ 235 MPa and from ~ 215 to ~ 265 MPa, respectively.

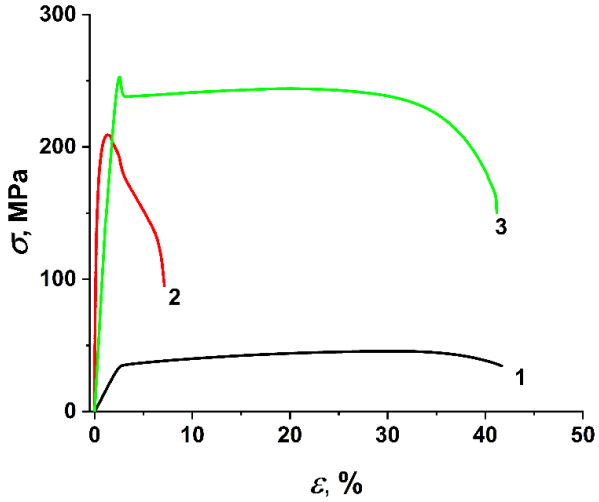

Fig. 2. Stress-strain curves of Al in the CG state (1) and in the UFG state Al_ECAP+CR+AN (2, 3) at RT (1, 2) and 77 K (3)

Figure 3 shows the stress-strain curves in true coordinates and the corresponding dependences of strain hardening coefficient ($\theta = d\sigma_{tr}/d\varepsilon_{tr}$, where σ_{tr} is true stress and ε_{tr} is true strain) on true strain for UFG Al in the Al_ECAP+CR+AN state at different deformation temperatures.

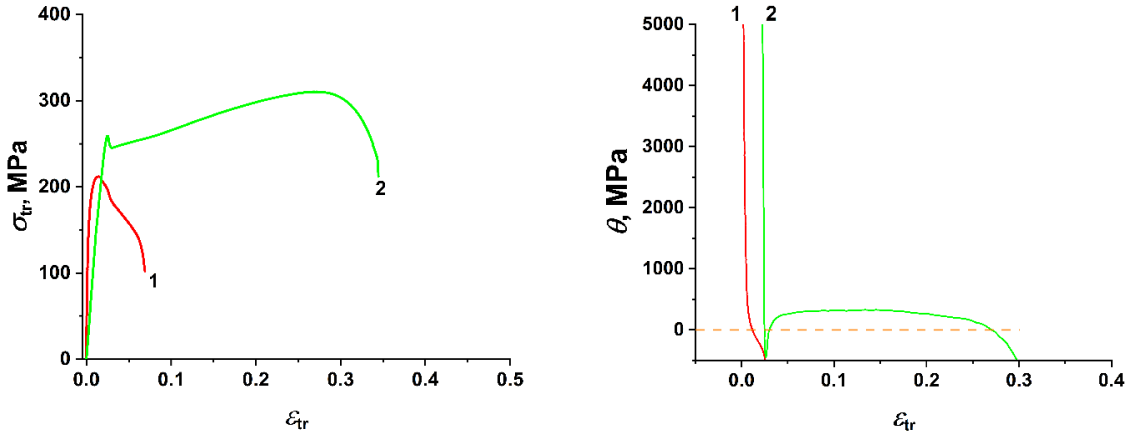

Fig. 3. (a) – true stress-strain curves of Al_ECAP+CR+AN at RT (curve 1) and 77 K (curve 2); (b) – the strain hardening coefficient as a function of true strain for Al_ECAP+CR+AN at RT (curve 1) and 77K (curve 2)

As is seen, the value of θ at RT sharply decreases to negative values when the strain is very small, that indicates low ability of UFG Al to strain hardening. At 77 K, the Al_ECAP+CR+AN samples show strain hardening ($\theta > 0$) until a large strain of ~ 25 % is reached (Fig. 3(b)). The high ductility of Al in the Al_ECAP+CR+AN state at 77 K opens up prospects for using this material to form products of complex shapes. High ductility at cryogenic temperature (77 K) was also demonstrated by UFG Al structured only by the CR method (Al_CR) [18]. However, Al_CR showed significantly lower strength at RT: $\sigma_{0.2}$ ~ 134 MPa and σ_{UTS} ~ 140 MPa, which are 1.35 and 1.5 times lower, respectively, than the such characteristics of Al_ECAP+CR+AN. At 77 K, both strength characteristics ($\sigma_{0.2}$ and σ_{UTS}) of Al_CR are also approximately 1.3 times lower than those of Al_ECAP+CR+AN. UFG

Al structured only by ECAP also has lower strength ($\sigma_{0.2}$ ~ 150 MPa and σ_{UTS} ~ 180 MPa) and low ductility (δ_1 ~ 3.9 % and δ ~ 14 %) at RT [19]. The yield stress of UFG Al samples structured by HPT is ~ 1.4 times lower compared to $\sigma_{0.2}$ of Al_ECAP+CR+AN samples. For UFG Al structured by HPT, no increase in ductility is observed at 77 K compared to that at RT [20]. At 77 K, the ductility of Al_HPT is δ ~ 19 % with uniform elongation δ_1 ~ 1 % in both states: with and without subsequent annealing at T = 150 °C for t = 1 h [20]. Thus, comparison of mechanical properties of Al_ECAP+CR+AN and UFG Al structured by other SPD methods at RT shows that the Al_ECAP+CR+AN samples have the best strength.

As is known, at large plastic deformation a subgrain structure develops in the initial CG material as a result of the rearrangement of dislocations accumulated during deformation [21,22]. When the strain reaches a critical value, the stationary regime of dynamic equilibrium of the nucleation and annihilation of dislocations is established, and a steady-state subgrain size w is reached. According to [23], the steady-state subgrain size is determined as:

$$w = k_w \frac{bG}{\sigma_{tr}^{max}}, \quad (1)$$

where k_w is a constant in the range 10–30, G is the shear modulus, b is the value of Burgers vector and σ_{tr}^{max} is the maximum true stress obtained from the stress-strain curves in true coordinates.

It is known that the value of the parameter w decreases with decreasing temperature and increasing strain rate [24,25]. At low temperatures, dynamic recovery (annihilation of dislocations and rearrangement of the dislocation structure) is suppressed, which contributes to a greater accumulation of dislocations during deformation. As a consequence, the free path of mobile dislocations decreases. The level of flow stress increases, that can promote the activation of additional sources of dislocations, leading to an overall increase in dislocation density. These dislocations can interact with each other and form a cell/subgrain dislocation structure with a lower w compared to the case of deformation at RT [24]. According to [18,22], the grain size d_G in a UFG structure relative to the parameter w at a given temperature and strain rate can play a decisive role in determining the overall deformation behavior of the material. In UFG alloys with a predominant grain size $d_G < w$, dislocations emitted from grain boundaries will glide to the opposite boundary (in the absence of any obstacles) and be embedded into it. Such dynamics of dislocations leads to a very slight or almost complete absence of strain hardening of the material, the rapid achievement of instability state (localization of deformation) in accordance with the Considère criterion: $\sigma = \theta$ [26,27], and, consequently, to low tensile ductility, primarily to low uniform elongation. In a UFG structure with a grain size $d_G > w$, emitted dislocations can interact with each other, accumulate, and form a cell/subgrain structure and, as a result, promote strain hardening.

In the present work, we estimated the parameter w for UFG Al_ECAP+CR+AN for deformation conditions at RT (w_{RT}) and 77 K (w_{77K}) according to Eq. (1). Using the values of G = 26 GPa at RT and 29.2 GPa at 77 K for Al [28], b = 0.286 nm [29] and the widely used value k_w = 20 for Al [30], as well as corresponding values of σ_{tr}^{max} determined from true stress – true strain diagrams (Fig. 3(a)), the values of $w_{RT} \approx 730$ nm and $w_{77K} \approx 530$ nm were obtained.

A comparison of the estimated w-values with the experimentally obtained grain size distribution for UFG Al in the Al_ECAP+CR+AN state (Fig. 1(b)) shows that the majority of

grains (fraction of grains $f \approx 65$ %) have a size d_G smaller then w_{RT}, therefore, at RT the accumulation of dislocations during deformation can occur mainly only in ~ 35 % of grains, that explains the low ductility at RT (Fig. 2). At the same time, the majority of grains (~ 75 %) meet the criterion $d_G > w_{77K}$; therefore, at 77 K, deformation with the accumulation of dislocations can occur in them promoting noticeable strain hardening, which is observed experimentally (Fig. 3) and explains the drastic increase in ductility at the cryogenic temperature (Fig. 2).

Conclusions

Thus, it was shown that UFG aluminium structured by a combination of ECAP and CR methods followed by annealing (T = 150 °C, t = 1 h) demonstrates drastic increase in ductility at 77 K compared with the ductility at RT. The values of δ and δ_1 increased respectively from ~ 10 % and ~ 1 % at RT to ~ 40 % and ~ 25 % at 77 K, while the strength also increased, reaching values of $\sigma_{0.2}$ ~ 235 MPa and σ_{UTS} ~ 265 MPa at 77 K. The achieved large uniform elongation opens up prospects for the use of cryogenic temperatures for molding products of complex shapes from such high-strength UFG aluminum, as well as its use for operation at cryogenic temperatures. It was shown that the increase in ductility, both elongation to failure and uniform elongation at 77 K, is associated with an increase in the strain hardening coefficient with decreasing deformation temperature and a high fraction of grains with sizes exceeding the characteristic steady-state subgrain size at 77 K.

References

1. Edalati K, Ahmed AQ, Akrami S, Ameyama K, Aptukov V, Asfandiyarov RN, Ashida M, Astanin V, Bachmaier A, Beloshenko V, Bobruk EV, Bryła K, Cabrera JM, Carvalho AP, Chinh NQ, Choi IC, Chulist R, Cubero-Sesin JM, Davdian G, Demirtas M, Zhu YT. Severe plastic deformation for producing superfunctional ultrafine-grained and heterostructured materials: An interdisciplinary review. *Journal of Alloys and Compounds*. 2024;1002: 174667.
2. Valiev RZ, Alexandrov IV, Kawasaki M, Langdon TG. *Ultrafine-Grained Materials*. Cham: Springer; 2024.
3. Karami S, Piroozi B, Borhani E. Fatigue-induced microstructure evolution and ratcheting behavior of ultrafine-grained (UFG) pure aluminum processed by accumulative roll bonding (ARB). *Materials Characterization*. 2023;196: 112578.
4. Lanjewar H, Naghdy S, Vercruysse F, Kestens LA, Verleysen P. Severe plastically deformed commercially pure aluminum: Substructure, micro-texture and associated mechanical response during uniaxial tension. *Materials Science and Engineering: A*. 2019;764: 138195.
5. Mohammadi A, Enikeev NA, Murashkin MYu, Arita M, Edalati K. Examination of inverse Hall-Petch relation in nanostructured aluminum alloys by ultra-severe plastic deformation. *Journal of Materials Science & Technology*. 2021;91: 78–89.
6. Evstifeev AD, Smirnov IV. Effect of annealing and additional deformation on the microstructure and mechanical properties of ultrafine-grained Al5083 alloy. *Materials Physics and Mechanics*. 2023;95(3): 20–28.
7. Edalati K, Bachmaier A, Beloshenko VA, Beygelzimer Y, Blank VD, Botta WJ, Bryła K, et al. Nanomaterials by severe plastic deformation: review of historical developments and recent advances. *Materials Research Letters*. 2022;10(4): 163–256.
8. Awasthi A, Sathish Rao U, Saxena KK, Dwivedi RK. Impact of equal channel angular pressing on aluminium alloys: An overview. *Materials Today: Proceedings*. 2022;57: 908–912.
9. Zhilyaev AP, Torres MJ, Cadena HD, Rodriguez SL, Calvo J, Cabrera JM. The effect of pre-annealing on the evolution of the microstructure and mechanical behavior of aluminum processed by a novel SPD method. *Materials*. 2020;13(10): 2361.
10. Chen X, Wang W, Wang M, Huang G, Zhang J, Pan F. Optimizing the strength and ductility of pure aluminum laminate via tailoring coarse/ultrafine grain layer thickness ratio. *Journal of Materials Research and Technology*. 2023;27: 7394–7406.

11. Huang T, Shuai L, Wakeel A, Wu G, Hansen N, Huang X. Strengthening mechanisms and Hall-Petch stress of ultrafine grained Al-0.3%Cu. *Acta Materialia.* 2018;156: 369–378.
12. Chen X, Wang W, Yang H, Huang G, Xia D, Tang A, Jiang B, Han HN, Pan F. Microstructure evolution, mechanical properties and deformation characteristics of ultrafine-grained annealed pure aluminum. *Materials Science and Engineering: A.* 2022;846: 143320.
13. Fu H, Zhou X, Xue H, Li X, Lu K. Breaking the purity-stability dilemma in pure Cu with grain boundary relaxation. *Materials Today.* 2022;55: 66–73.
14. Mavlyutov AM, Latynina TA, Murashkin MYu, Valiev RZ, Orlova TS. Effect of annealing on the microstructure and mechanical properties of ultrafine-grained commercially pure Al. *Physics of the Solid State.* 2017;59(10): 1970–1977.
15. Orlova TS, Skiba NV, Mavlyutov AM, Valiev RZ, Murashkin MY, Gutkin MY. Hardening by annealing and implementation of high ductility of ultra-fine grained aluminum: experiment and theory. *Reviews On Advanced Materials Science.* 2018;57(2): 224–240.
16. Orlova TS, Sadykov DI, Kirilenko DA, Lihachev AI, Levin AA. The key role of grain boundary state in deformation-induced softening effect in Al processed by high pressure torsion. *Materials Science and Engineering: A.* 2023;875: 145122.
17. Sadykov DI, Medvedev AE, Murashkin MYu, Enikeev NA, Kirilenko DA, Orlova TS. Influence of ultrafine-grained structure parameters on the annealing-induced hardening and deformation-induced softening effects in pure Al. *International Journal of Lightweight Materials and Manufacture.* 2024;7(2): 221–232.
18. Wang R, Liu W, Hao Y, Yao M. Mechanism of considerable strain hardening in ultrafine-grained pure aluminum sheets at cryogenic temperatures. *Materials Science and Engineering: A.* 2023;862: 144481.
19. Yu CY, Sun PL, Kao PW, Chang CP. Mechanical properties of submicron-grained aluminum. *Scripta Materialia.* 2005;52(5): 359–363.
20. Orlova TS, Mavlyutov AM, Gutkin MYu. Suppression of the annealing-induced hardening effect in ultrafine-grained Al at low temperatures. *Materials Science and Engineering: A.* 2021;802: 140588.
21. Tian YZ, Gao S, Zhao LJ, Lu S, Pippan R, Zhang ZF, Tsuji N. Remarkable transitions of yield behavior and Lüders deformation in pure Cu by changing grain sizes. *Scripta Materialia.* 2018;142: 88–91.
22. Kumar N, Mishra RS, Huskamp CS, Sankaran KK. Critical grain size for change in deformation behavior in ultrafine grained Al–Mg–Sc alloy. *Scripta Materialia.* 2011;64(6): 576–579.
23. Li YJ, Zeng XH, Blum W. Transition from strengthening to softening by grain boundaries in ultrafine-grained Cu. *Acta Materialia.* 2004;52(17): 5009–5018.
24. Huang F, Tao NR. Effects of strain rate and deformation temperature on microstructures and hardness in plastically deformed pure aluminum. *Journal of Materials Science & Technology.* 2011;27(1): 1–7.
25. Huang Y, Prangnell PB. The effect of cryogenic temperature and change in deformation mode on the limiting grain size in a severely deformed dilute aluminium alloy. *Acta Materialia.* 2008;56(7): 1619–1632.
26. Kozlov EV, Glazer AM, Koneva NA, Popova NA, Kurzina IA. *Fundamentals of plastic deformation of nanostructured materials.* Moscow: FIZMATLIT; 2016. (In Russian)
27. Backofen WA. *Deformation processing.* Boston: Addison-Wesley Educational Pub; 1972.
28. Cheng W, Liu W, Fan X, Yuan S. Cooperative enhancements in ductility and strain hardening of a solution-treated Al–Cu–Mn alloy at cryogenic temperatures. *Materials Science and Engineering: A.* 2020;790: 139707.
29. Anderson PM, Hirth JP, Lothe J. *Theory of dislocations.* 3rd ed. Cambridge: Cambridge University Press; 2017.
30. Wang BB, Xie GM, Wu LH, Xue P, Ni DR, Xiao BL, Liu YD, Ma ZY. Grain size effect on tensile deformation behaviors of pure aluminum. *Materials Science and Engineering: A.* 2021;820: 141504.

About Author

Tatiana S. Orlova Sc
Doctor of Physical and Mathematical Sciences
Principal Researcher (Ioffe Institute, St. Petersburg, Russia)

Dinislam I. Sadykov Sc
Junior Researcher (Ioffe Institute, St. Petersburg, Russia)